separations

MDPI

Article

Analysis of Oligopeptides from Pilose Antler Using Tandem Mass Tags Combined with Ultra-High-Performance Liquid Chromatography-Q-Orbitrap/Mass Spectrometry

Shengyu Ge [1], Muran Deng [1], Hailin Zhu [2,*] and Lele Li [1,*]

[1] School of Pharmacy, Jilin Medical University, Jilin 132013, China
[2] School of Pharmacy, Nanchang University, Nanchang 330000, China
* Correspondence: zhuhailin2020@ncu.edu.cn (H.Z.); lilele19911006@163.com (L.L.); Tel./Fax: +86-431-8676-3990 (H.Z.); +86-432-6456-0316 (L.L.)

Abstract

Reports on oligopeptides derived from pilose antler remain scarce. There is an urgent need to establish a robust analytical method for detecting and characterizing these compounds. In this study, oligopeptide extracts from pilose antler were labeled with tandem mass tag (TMT) reagents and analyzed using ultra-high-performance liquid chromatography coupled with Q-Orbitrap/mass spectrometry (UHPLC-Q-Orbitrap/MS). Amino acid profiles and oligopeptide sequences were determined from accurate m/z values and tandem mass information. Twenty-six amino acids and 33 oligopeptides were identified in pilose antler extracts. The integrated TMT and UHPLC-Q-Orbitrap/MS approach enabled comprehensive analysis of oligopeptides and amino acids, establishing a foundation for holistic quality assessment of pilose antler oligopeptides.

Keywords: pilose antler; oligopeptides; high-resolution mass spectrometry; stable isotope labeling; amino acid

1. Introduction

Pilose antler, a traditional Chinese medicine employed for millennia in China as a natural remedy or tonic food, enhances renal function, strengthens tendons and bones, and prolongs lifespan [1–3]. Polypeptides are recognized as the primary bioactive compounds responsible for most pharmacological effects of pilose antler, and their structures and bioactivities have been extensively investigated over recent decades [4–8]. Recent studies have demonstrated that pilose antler oligopeptides can promote the proliferation of mouse osteoblasts [9]. In addition, pilose antler oligopeptides have been employed as key ingredients in enteric-coated microcapsules for the intervention of kidney yang deficiency syndrome [10]. Nevertheless, oligopeptides from pilose antler remain poorly characterized, and only limited information is available regarding their structural features and biological functions. Therefore, it is necessary to develop efficient analytical approaches to profile pilose antler oligopeptides and further clarify their structure–activity relationships.

Oligopeptides, defined as short peptide chains comprising 2–10 amino acids linked by peptide bonds, represent an intermediate category between simple amino acids and complex polypeptides or proteins [11]. Their low molecular weight (typically < 10 kDa) enhances intestinal epithelial permeability and bioavailability compared to larger proteins. Consequently, research on pilose antler oligopeptides provides direct insights into the bioactive and pharmacological properties of this medicinal material.

Check for updates

Academic Editor: Shun Yao

Received: 6 September 2026
Revised: 5 October 2026
Accepted: 5 October 2026
Published: 8 October 2026

Copyright: © 2026 by the authors. Licensee MDPI, Basel, Switzerland. This article is an open access article distributed under the terms and conditions of the Creative Commons Attribution (CC BY) license.

Tandem mass tags (TMT) technology is the most commonly used stable isotope labeling technique in quantitative proteomics [12,13]. It can achieve simultaneous and precise qualitative and quantitative analysis of multiple samples through multiple pathways. It involves labeling the oligopeptide segments obtained by enzymatic digestion of proteins with TMT isotope reagents. The labeling sites are the N-terminus of the oligopeptide segments. The labeled oligopeptide segments are then subjected to liquid-phase separation and undergo accurate m/z value and tandem mass information. In the MS spectra, the same oligopeptide segment in different labeled samples exhibits the same m/z and physicochemical properties. In the MS/MS spectra, the amide bonds of the oligopeptides break, and the reporter ions appear as peaks with different m/z ratios (126–135). The height and area of the peaks can reflect the relative abundance of the same oligopeptide in different samples, thereby enabling quantification. At the same time, a series of y-ions and b-ions are formed. Analysis of the series of fragment ions can provide structural information about the corresponding oligopeptide. Compared with label-free approaches, TMT isobaric labeling enables the reporter ion signals to assist in filtering false positive identifications. In addition, TMT-modified oligopeptides exhibit improved proton affinity and can generate enhanced MS signals. Accordingly, the TMT labeling strategy was adopted for oligopeptide identification in the present study.

Here, we report a method combining TMT with ultra-high-performance liquid chromatography-Q-Orbitrap/mass spectrometry (UHPLC-Q-Orbitrap/MS) for the analysis of pilose antler oligopeptides. The identification of pilose antler oligopeptides is mainly achieved by analyzing the accurate m/z values and tandem mass spectra of TMT-labeled oligopeptides. In addition, we also identified amino acids in pilose antler. The workflow of this study and the TMT labeling reaction process are illustrated in Figure S1.

2. Materials and Methods

2.1. Chemical Reagents and Materials

HPLC-grade acetonitrile, methanol, and formic acid were purchased from TEDIA (Fairfield, OH, USA). Ultra-pure water was processed by the Milli-Q water purification system (Millipore, Bedford, MA, USA).The TMTsixplex isobaric label reagent set (Contains 6 types of TMT labeling reagents with corresponding reporter ions of 126, 127, 128, 129, 130, and 131) was obtained from Thermo Fisher Scientific (San Jose, CA, USA). Ultrafiltration centrifuge tubes ($\leq$3 kDa) were purchased from Millipore (Bedford, MA, USA). Three batches of pilose antler samples from *Cervus elaphus* Linnaeus were purchased from a local market in 2024. Three batches of pilose antler decoction pieces (*Cervus elaphus* Linnaeus) were purchased from a local pharmaceutical company. Detailed information on the samples is shown in Table 1. The above-mentioned pilose antler decoction pieces were identified as authentic by Professor Jinghua Li from the Department of Chinese Materia Medica, Jilin Medical University, Jilin. γ-aminobutyric acid, α-aminobutyric acid, leucine, and isoleucine standards were purchased from Solarbio Science & Technology Co., Ltd. (purity $\geq$ 98%, Beijing, China). Ile-Glu, Leu-Glu, Gly-Ile, Gly-Leu, Ile-Hyp, Leu-Hyp, Glu-Ile, Glu-Leu, Ile-Pro, Val-Ile, Leu-Pro, Val-Leu, Val-Leu-Ser-Ala, Val-Gly-Ile, Val-Gly-Leu, Ile-Leu, Leu-Ile, Leu-Leu, Phe-Leu, Phe-Asp-Leu standards were provided by Sangon Biotech (Shanghai) Co., Ltd. (purity $\geq$ 95%, Beijing, China). A BCA protein assay kit was purchased from Shanghai Yuanye Bio-Technology Co., Ltd. (Shanghai, China).

Table 1. Chemical information of amino acids in pilose antler.

Amino Acid (Abbreviation)	Molecular Formula	Mass	Amino Acid Residue		RT (min)	*m/z*	Mass Error (ppm)	Sample 1	Sample 2	Sample 3
			Molecular Formula	Mass						
Histidine (His)	$C_6H_9N_3O_2$	155.0689	$C_6H_7N_3O$	137.0583	0.82	385.2394	−0.52	+	+	+
Arginine (Arg)	$C_6H_{14}N_4O_2$	174.1105	$C_6H_{12}N_4O$	156.1005	0.87	404.2806	−1.48	+	+	+
Serine (Ser)	$C_3H_7NO_3$	105.0414	$C_3H_5NO_2$	87.0314	1.10	335.2124	0.89	+	+	+
Glycine (Gly)	$C_2H_5NO_2$	75.0309	C_2H_3NO	57.0209	1.23	305.2013	−0.98	+	+	+
Asparagine (Asn)	$C_4H_8N_2O_3$	132.0523	$C_4H_6N_2O_2$	114.0423	1.45	362.2217	−3.59	+	+	+
Taurine (Tau)	$C_2H_7NO_3S$	125.0135	$C_2H_5NO_2S$	107.0035	1.77	355.1836	−1.68	+	+	+
Glutamine (Gln)	$C_5H_{10}N_2O_3$	146.0680	$C_5H_8N_2O_2$	128.0580	1.96	376.2375	−3.19	+	+	+
Aspartic acid (Asp)	$C_4H_7NO_4$	133.0363	$C_4H_5NO_3$	115.0263	2.08	363.2065	−1.37	+	+	+
Hydroxyproline(Hyp)	$C_5H_9NO_3$	131.0577	$C_5H_7NO_2$	113.0471	2.41	361.2275	−2.49	+	+	+
Glutamic acid (Glu)	C5H9NO$_4$	147.0520	$C_5H_7NO_3$	129.0420	2.66	377.2217	−2.65	+	+	+
Threonine (Thr)	$C_4H_9NO_3$	119.0571	$C_4H_7NO_2$	101.0471	2.88	349.2274	−1.14	+	+	+
Alanine (Ala)	$C_3H_7NO_2$	89.0465	C_3H_5NO	71.0365	2.98	319.2162	−3.13	+	+	+
γ-aminobutyric acid (Gaba)	$C_4H_9NO_2$	103.0622	C_4H_7NO	85.0522	5.94	333.2327	−0.60	+	+	+
α-aminobutyric acid (Aaba)	$C_4H_9NO_2$	103.0622	C_4H_7NO	85.0522	7.40	333.2316	−3.90	+	+	+
Hydroxylysine (Hyl)	$C_6H_{14}N_2O_3$	162.0993	$C_6H_{12}N_2O_2$	144.0893	7.48	392.2681	−4.84	+	+	+
Proline (Pro)	$C_5H_9NO_2$	115.0622	C_5H_7NO	97.0522	7.99	345.2325	−1.16	+	+	+
Methionine (Met)	$C_5H_{11}O_2NS$	149.0499	C_5H_9ONS	131.0399	8.89	379.2208	0.53	+	+	+
Valine (Val)	$C_5H_{11}NO_2$	117.0778	C_5H_9NO	99.0678	9.67	347.2478	−2.02	+	+	+
Tyrosine (Tyr)	$C_9H_{11}NO_3$	181.0727	$C_9H_9NO_2$	163.0627	10.06	411.2418	−3.89	+	+	+
Ornithine (Orn)	$C_5H_{12}N_2O_2$	132.0887	$C_5H_{10}N_2O$	114.0787	13.76	362.2579	−0.41	+	+	+
Isoleucine(Ile)	$C_6H_{13}NO_2$	131.0935	$C_6H_{11}NO$	113.0835	14.11	361.2627	−4.15	+	+	+
Leucine(Leu)	$C_6H_{13}NO_2$	131.0935	$C_6H_{11}NO$	113.0835	14.82	361.2626	−4.43	+	+	+
Phenylalanine(Phe)	$C_9H_{11}NO_2$	165.0778	C_9H_9NO	147.0678	17.28	395.2473	−3.04	+	+	+
Lysine (Lys)	$C_6H_{14}N_2O_2$	146.1044	$C_6H_{12}N_2O$	128.0944	19.73	376.2744	−1.86	+	+	+
Tryptophan(Trp)	$C_{11}H_{12}N_2O_2$	204.0887	$C_{11}H_{10}N_2O$	186.0787	20.10	434.2574	−4.61	+	+	+
Cysteine (Cys)	$C_3H_7NO_2S$	121.0186	C_3H_5NOS	103.0086	22.42	351.1881	−3.42	+	+	+

+, the corresponding amino acid was detected in the sample; −, not detected.

2.2. Sample Extraction

The pilose antler decoction pieces were crushed and passed through a 20-mesh sieve. One gram of powdered sample was immersed in 20 mL of water for 1 h and extracted using a magnetic mixer at 600 rpm at 60 °C for 2 h. Extraction was performed at a relatively low temperature instead of the conventional boiling method widely adopted for traditional Chinese medicine extraction. The primary purpose of this strategy was to avoid the hydrolysis of some proteins or polypeptides, which could generate new oligopeptides and thereby interfere with the identification of intrinsic oligopeptide components in pilose antler. The extract was centrifuged for 10 min at 6000 rpm. The supernatant was collected and concentrated to 5 mL. The concentrated solution was filtered using ultrafiltration centrifuge tubes ($\leq$3 kDa) at 12,000 rpm, and the filtrate was concentrated by vacuum centrifugation at 2000 rpm to obtain pilose antler oligopeptide extract. Three batches of pilose antler decoction pieces derived from different sources were extracted according to the aforementioned method, yielding the corresponding extracts. The obtained pilose antler oligopeptide samples weighed 1.59 $\pm$ 0.28 mg.

An appropriate amount of pilose antler oligopeptide sample was dissolved in water. The protein-equivalent concentration of the resulting sample solution was determined using a BCA protein assay kit. The protein-equivalent content of the pilose antler oligopeptide sample was 63.28 $\pm$ 4.71%.

2.3. Labeling Oligopeptides with the TMT Isobaric Mass Tags

Forty-one μL of anhydrous acetonitrile was added to each TMT label reagent tube. The reagent was allowed to dissolve for 5 min with occasional vortexing. Then, the tube was briefly centrifuged to gather the solution. Triethylammonium bicarbonate buffer (100 mM) was added to the pilose antler oligopeptide extract for redissolution. Approximately 1 mg of pilose antler oligopeptide extract was weighed and dissolved in 500 μL of water. An aliquot of the reconstituted solution (equivalent to 100 μg of protein) was mixed with 41 μL of TMTsixplex-126 labeling reagent, followed by incubation at 25 °C for 1 h. Eight μL of 5% hydroxylamine was added to the mix solution, which was then incubated for 15 min to quench the reaction. All three pilose antler oligopeptide extract samples were processed following the above-described procedure. The prepared samples were analyzed by UHPLC-Q-Orbitrap/MS.

Leucine, α-aminobutyric acid, and the oligopeptides containing leucine were all labeled with TMTsixplex-127. Isoleucine, γ-aminobutyric acid, and the oligopeptides containing isoleucine were all labeled with TMTsixplex-128. All the labeled standards were mixed and then analyzed by UHPLC-Q-Orbitrap/MS.

2.4. UHPLC-Q-Orbitrap/MS Analysis

Ultra-high-performance liquid chromatography (UHPLC) was performed on an UltiMate 3000 system (Dionex, Sunnyvale, CA, USA) coupled with a Hypersill Gold C18 column (2.1 × 50 mm, 1.9 μm; Thermo Fisher Scientific, San Jose, CA, USA) maintained at 40 °C. Mobile phase A consisted of 0.1% (*v*/*v*) formic acid in water, and mobile phase B was 100% acetonitrile. The gradient program for mobile phase B was as follows: 0.1% (0–1 min), 0.1% to 10% (1–20 min), 10% to 50% (20–40 min), 50% to 95% (40–43 min), 95% (43–47 min), and 95% to 5% (47–47.1 min). The system was subsequently equilibrated at 5% B for 2.9 min. The injection volume was 5.0 μL per sample, and the flow rate was 0.4 mL/min.

Mass spectrometric detection was conducted on a Q Exactive Orbitrap MS (Thermo Fisher Scientific) equipped with an electrospray ionization (ESI) source operated in positive-ion mode. The MS parameters were set as follows: sheath gas flow, 40 arb; auxiliary gas flow, 12 arb; sweep gas flow, 1 arb; capillary voltage, +3.5 kV; capillary temperature,

333 °C; auxiliary gas heater temperature, 317 °C. Full-scan MS (MS^1) data were acquired in positive-ion mode across m/z 100–1500 with a resolution of 70,000 (at m/z 200), an AGC target of 1×10^3, and a maximum injection time of 100 ms. Data-dependent MS/MS ($ddMS^2$, Top 10) spectra were acquired with a resolution of 17,500 (at m/z 200), an AGC target of 1×10^3, a maximum injection time of 50 ms, and a precursor isolation width of 4 Da. Fragmentation was performed using a normalized collision energy of 40% combined with stepped collision energies of 20%. Data acquisition and analysis were performed using Xcalibur software (version 2.2.42, Thermo Fisher Scientific).

3. Results

3.1. Identification of Amino Acids

Figure 1 displays the representative total ion chromatogram (TIC) of the TMT-labeled pilose antler sample (sample 1). Only amino acids or oligopeptides that were detected in at least two out of the three pilose antler sample batches were identified and annotated in Figure 1. Prior to oligopeptide identification, the amino acid profile in pilose antler was characterized. With the exception of γ-aminobutyric acid, α-aminobutyric acid, leucine, and isoleucine, all amino acids were identified using MS and MS/MS data. Glycine served as a representative example for validation. The compound at a retention time of 1.23 min exhibited an m/z of 305.2013 (Figure 2A), showing a minimal mass error (2.24 ppm) relative to the theoretical m/z of TMT-labeled glycine. The MS/MS spectrum (Figure 2B) revealed a reporter ion at m/z 126.1275 (theoretical m/z: 126.1278). A diagnostic product ion at m/z 230.1684, with a 75.0329 Da mass difference from the precursor ion (m/z 305.2013), confirmed the presence of glycine.

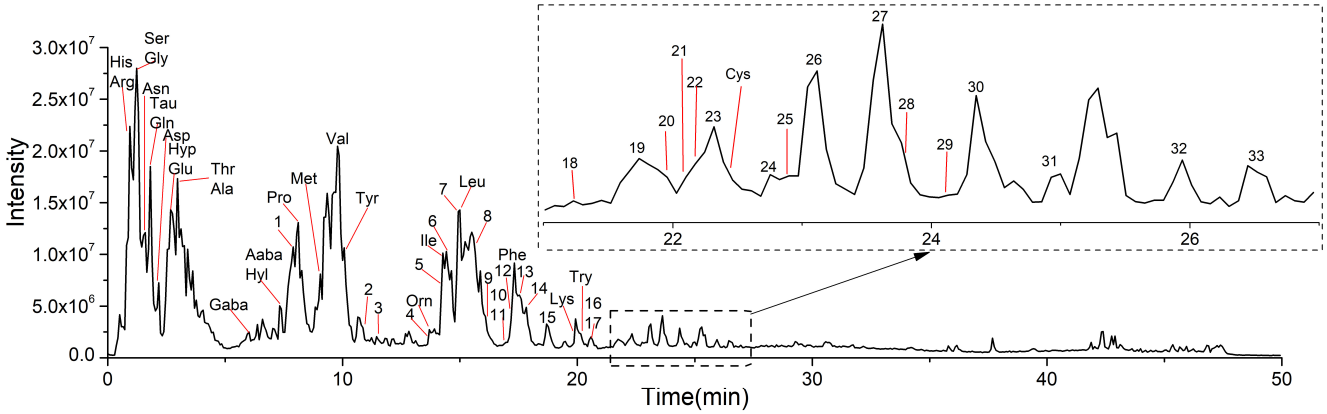


Figure 1. Representative total ion chromatograms (TIC) of the TMT-labeled pilose antler extracts. (1, 2, 3... the numbers representing the corresponding oligopeptides are provided in Table 2).

Leucine, isoleucine, γ-aminobutyric acid, and α-aminobutyric acid were identified by comparison with TMT-labeled standards (Figure S2). Collectively, 26 amino acids were characterized in pilose antler, with complete chemical profiles detailed in Table 1. The identified amino acids are consistent with the previous reports [14,15].

Table 2. Identification results of pilose antler oligopeptides.

No.	Amino Acid Sequence	RT (min)	Adducts	Precursor Ions			Product Ions		Sample 1	Sample 2	Sample 3
				Theoretical *m*/*z*	Observed *m*/*z*	Mass Error (ppm)	Theoretical *m*/*z* (Ion Name)	Observed *m*/*z* (Ion Name, Mass Error ppm)			
1	Gly-Pro-Hyp	7.74	$[M+H]^+$	515.3009	515.3000	−1.75	259.1961 (a1), 287.1910 (b1), 384.2432 (b2)	259.1953 (a1, −3.08), 287.1909 (b1, −0.35), 384.2422 (b2, −2.60)	+	+	+
2	Ala-Val	10.94	$[M+H]^+$	418.2850	418.2841	−2.15	273.2117 (a1), 301.2066 (b1)	273.2131 (a1, 5.12), 301.2081 (b1, 4.97)	+	+	+
3	Ala-Tyr	11.8	$[M+H]^+$	482.2799	482.2795	−0.83	301.2066 (b1)	301.2076 (b1, 3.31)	+	+	+
4	Ile-Glu *	13.58	$[M+H]^+$	490.3062	490.3048	−2.86	315.2587 (a1), 343.2536 (b1)	315.2612 (a1, 7.93), 343.2546 (b1, 2.91)	+	–	+
5	Leu-Glu *	14.06	$[M+H]^+$	490.3062	490.3044	−3.67	315.2587 (a1), 343.2536 (b1)	315.2601 (a1, 2.91), 343.2556 (b1, 5.82)	+	+	+
6	Gly-Ile *	14.27	$[M+H]^+$	418.2851	418.2836	−3.59	259.1961 (a1), 287.1910 (b1)	259.1969 (a1, 3.09), 287.1930 (b1, 6.96)	+	+	+
7	Gly-Leu *	14.85	$[M+H]^+$	418.2851	418.2839	−2.87	259.1961 (a1), 287.1910 (b1)	259.1953 (a1, −3.08), 287.1926 (b1, 5.57)	+	+	+
8	Ile-Hyp *	15.67	$[M+H]^+$	474.3113	474.3091	−4.64	315.2587 (a1), 343.2536 (b1)	315.2571 (a1, −5.08), 343.2526 (b1, −2.91)	+	+	+
9	Leu-Hyp *	16.13	$[M+H]^+$	474.3113	474.3103	−2.11	315.2587 (a1), 343.2536 (b1)	315.2571 (a1, −5.08), 343.2517 (b1, −5.54)	+	+	+
10	Glu-Ile *	16.74	$[M+H]^+$	490.3062	490.3052	−2.04	331.2172 (a1), 359.2121 (b1)	331.2195 (a1, 6.94), 359.2141 (b1, 5.57)	+	+	+
11	Ser-Phe	16.74	$[M+H]^+$	482.2799	482.2808	1.87	289.2066 (a1), 317.2015 (b1)	289.2069 (a1, 1.04), 317.2013 (b1, −0.63)	+	+	+
12	Gly-Phe	16.94	$[M+H]^+$	452.2694	452.2680	−3.10	259.1961 (a1), 287.1910 (b1)	259.1969 (a1, 3.09), 287.1932 (b1, 7.66)	+	+	+
13	Glu-Leu *	17.57	$[M+H]^+$	490.3062	490.3048	−2.86	331.2172 (a1), 359.2121 (b1)	331.2166 (a1, −1.81), 359.2108 (b1, −3.62)	+	+	+
14	Phe-Hyp	17.98	$[M+H]^+$	508.2956	508.2933	−4.52	349.2430 (a1), 377.2379 (b1)	349.2422 (a1, −2.29), 377.2385 (b1, 1.59)	+	+	+
15	Ala-Phe	18.63	$[M+H]^+$	466.285	466.2847	−0.64	273.2117 (a1), 301.2066 (b1)	273.2106 (a1, −4.03), 301.2051 (b1, −4.98)	+	+	+
16	Ala-Trp	20.83	$[M+H]^+$	505.2959	505.2946	−2.57	273.2117 (a1), 301.2066 (b1)	273.2126 (a1, 3.29), 301.2084 (b1, 2.66)	+	+	+
17	Ile-Pro *	21	$[M+H]^+$	458.3164	458.3154	−2.18	315.2587 (a1), 343.2536 (b1)	315.2540 (a1, −1.49), 343.2618 (b1, −5.24)	+	+	+
18	Val-Ile *	21.4	$[M+H]^+$	460.3320	460.3307	−2.82	301.2430 (a1), 329.2379 (b1)	301.2440 (a1, 3.32), 329.2395 (b1, 4.86)	+	+	+
19	Leu-Pro *	21.78	$[M+H]^+$	458.3164	458.3160	−0.87	315.2587 (a1), 343.2536 (b1)	315.2570 (a1, −5.39), 343.2618 (b1, −2.33)	+	+	+

Table 2. *Cont.*

No.	Amino Acid Sequence	RT (min)	Adducts	Precursor Ions			Product Ions		Sample 1	Sample 2	Sample 3
				Theoretical *m*/*z*	Observed *m*/*z*	Mass Error (ppm)	Theoretical *m*/*z* (Ion Name)	Observed *m*/*z* (Ion Name, Mass Error ppm)			
20	Gly-Pro-Hyp-Gly-Phe	21.96	$[M+H]^+$	719.3896	719.3892	−0.56	259.1961 (a1), 287.1910 (b1), 384.2432 (b2), 497.2903 (b3), 526.3163 (a4), 554.3112 (b4)	259.1954 (a1, −2.70), 287.1908 (b1, −0.70), 356.2482 (a2, −0.28), 384.2436 (b2, 1.04), 497.2914 (b3, 2.21), 526.3176 (a4, 2.47), 554.3097 (b4, −2.71)	+	+	+
21	Val-Leu *	22.05	$[M+H]^+$	460.3320	460.3316	−0.87	301.2430 (a1), 329.2379 (b1)	301.2427 (a1, −1.00), 329.2465 (b1, −4.25)	+	+	+
22	Val-Leu-Ser-Ala *	22.16	$[M+H]^+$	618.3999	618.3988	−1.78	301.2430 (a1), 329.2379 (b1), 414.3265 (a2), 442.3214 (b2), 529.3528 (b3)	301.2419 (a1, −3.65), 329.2364 (b1, −4.56), 414.3230 (a2, −8.45), 442.3184 (b2, −6.78), 529.3497 (b3, −5.86)	+	+	+
23	Val-Gly-Ile *	22.25	$[M+H]^+$	517.3529	517.3523	−1.16	301.2430 (a1), 329.2379 (b1), 358.2639 (a2), 386.2588 (b2)	301.2433 (a1, 0.99), 329.2369 (b1, −3.04), 358.2632 (a2, −1.95), 386.2592 (b2, 1.04)	+	+	+
24	Gly-Asp-Phe-Tyr	22.76	$[M+H]^+$	730.3584	730.3570	−1.92	259.1961 (a1), 287.1910 (b1), 402.2173 (b2), 521.2902 (a3), 549.2851 (b3)	259.1956 (a1, −1.95), 287.1910 (b1, 0.00), 402.2149 (b2, −5.97), 521.2891 (a3, −2.11), 549.2841 (b3, −1.82)	+	+	+
25	Val-Gly-Leu *	22.9	$[M+H]^+$	517.3529	517.3507	−4.25	301.2430 (a1), 329.2379 (b1), 358.2639 (a2), 386.2588 (b2)	301.2441 (a1, 3.65), 329.2440 (b1, 3.04), 358.2391 (a2, −5.02), 386.2674 (b2, −3.62)	+	–	+
26	Phe-Pro	23.23	$[M+H]^+$	492.3007	492.2990	−3.45	377.2379 (b1)	377.2385 (b1, 1.59)	+	+	+
27	Glu-Pro	23.76	$[M+H]^+$	474.2749	474.2748	−2.11	331.2172 (a1), 359.2121 (b1)	331.2193 (a1, 6.34), 359.2138 (b1, 4.73)	+	+	+
28	Val-Asn-Phe	23.96	$[M+H]^+$	608.3589	608.3569	−3.29	301.2430 (a1), 329.2379 (b1)	301.2446 (a1, 5.31), 329.2354 (b1, −7.59), 443.2783 (b1, −4.29)	+	+	+
29	Ile-Leu *	24.06	$[M+H]^+$	474.3477	474.3467	−2.11	315.2587 (a1), 343.2536 (b1)	315.2576 (a1, −3.50), 343.2532 (b1, −1.17)	+	+	–
30	Leu-Ile *	24.49	$[M+H]^+$	474.3477	474.3463	−2.95	315.2587 (a1), 343.2536 (b1)	315.2575 (a1, −3.81), 343.2521 (b1, −4.37)	+	+	+
31	Leu-Leu *	24.91	$[M+H]^+$	474.3477	474.3460	−3.58	315.2587 (a1), 343.2536 (b1)	315.2584 (a1, −0.95), 343.2516 (b1, −5.83)	+	+	+

Table 2. *Cont.*

No.	Amino Acid Sequence	RT (min)	Adducts	Precursor Ions			Product Ions		Sample 1	Sample 2	Sample 3
				Theoretical *m*/*z*	Observed *m*/*z*	Mass Error (ppm)	Theoretical *m*/*z* (Ion Name)	Observed *m*/*z* (Ion Name, Mass Error ppm)			
32	Phe-Leu *	25.91	$[M+H]^+$	508.332	508.3301	−3.73	349.2430 (a1), 377.2379 (b1)	349.2423 (a1, −2.00), 377.2370 (b1, −2.39)	+	+	+
33	Phe-Asp-Leu *	26.5	$[M+H]^+$	623.3583	623.3571	−1.92	349.2430 (a1), 377.2379 (b1)	349.2432 (a1, 0.57), 377.2372 (b1, −1.86), 492.2620 (b2, −4.67)	+	+	+

*: The oligopeptides was identified using the standards; +, the corresponding oligopeptide was detected in the sample; −, not detected.

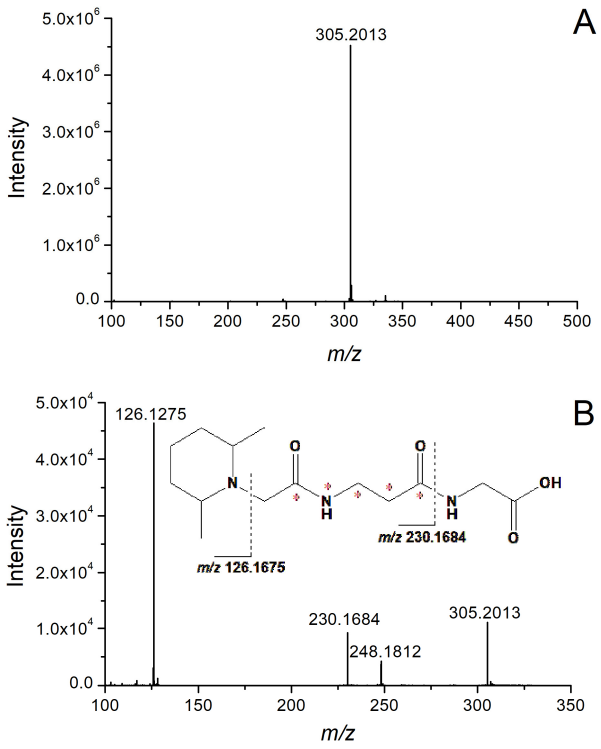


Figure 2. MS (**A**) and MS/MS (**B**) spectra of TMT-labeled glycine. (*: The carbon atom at this position is substituted with ^{13}C).

3.2. Identification of Oligopeptides

The identification results of oligopeptides are presented in Figure 1 and Table 2. Thirty-three oligopeptides (comprising two to five amino acid residues) were identified in pilose antler. For oligopeptides lacking leucine or isoleucine, identification was accomplished via diagnostic MS fragmentation patterns.

The identification process is exemplified using oligopeptide 24 (Gly-Asp-Phe-Tyr). The precursor ion for this oligopeptide was observed at *m*/*z* 730.3574, and its MS/MS spectrum is shown in Figure 3A. In addition to the reporter ion, the spectrum contained b-type ions (*m*/*z* 287.1910, 402.2149, 549.2881), a-type ions (*m*/*z* 259.1956, 521.2831), and other ions (*m*/*z* 420.2243, 567.2973). The b-type ions are instrumental in determining the amino acid sequence. Specifically, the b3 ion at *m*/*z* 549.2881 corresponds to the precursor ion minus 181.0693, supporting the presence of a C-terminal tyrosine residue (theoretical mass: 181.0727). Loss of a phenylalanine residue (theoretical mass: 147.0678) from the b3 ion (*m*/*z* 549.2881) yielded the b_2 ion at *m*/*z* 402.2149. Subsequent loss of an aspartic acid residue (theoretical mass: 115.0263) from the b2 ion produced the b1 ion at *m*/*z* 287.1910. The mass difference of 57.0212 between *m*/*z* 230.1698 (an ion derived from the TMT tagging group) and the b1 ion (*m*/*z* 287.1910) indicates an N-terminal glycine residue. The a-type ions, resulting from CO loss from b-type ions, provide complementary information for sequence assignment.

Oligopeptide 1 (Gly-Pro-Hyp) further exemplifies this identification process In Proceedings of the (Figure 3B). Its precursor ion was observed at *m*/*z* 515.2999, with the MS/MS spectrum revealing b-type ions (*m*/*z* 287.1909, 384.2422), a-type ions (*m*/*z* 259.1953), and y-type ions (*m*/*z* 132.0646, 229.1174). While a- and b-type ions are primary determinants of the amino acid sequence, y-type ions provide complementary evidence. The b2 ion at *m*/*z* 384.2422 arose from a mass loss of 131.0577 Da from the precursor ion. Although hydroxyproline, leucine, and isoleucine share similar nominal masses (~131 Da), the high resolving power of the Q-Orbitrap/MS platform enabled precise differentiation.

The measured fragment mass of 131.0577 Da corresponds to hydroxyproline (theoretical mass: 131.0576 Da) and unequivocally excludes leucine and isoleucine (theoretical mass: 131.0935 Da; Δm = 35.8 ppm), confirming hydroxyproline as the C-terminal residue. Additional ions collectively supported the identification of proline and glycine residues within the sequence (detailed annotations in Figure 3B).

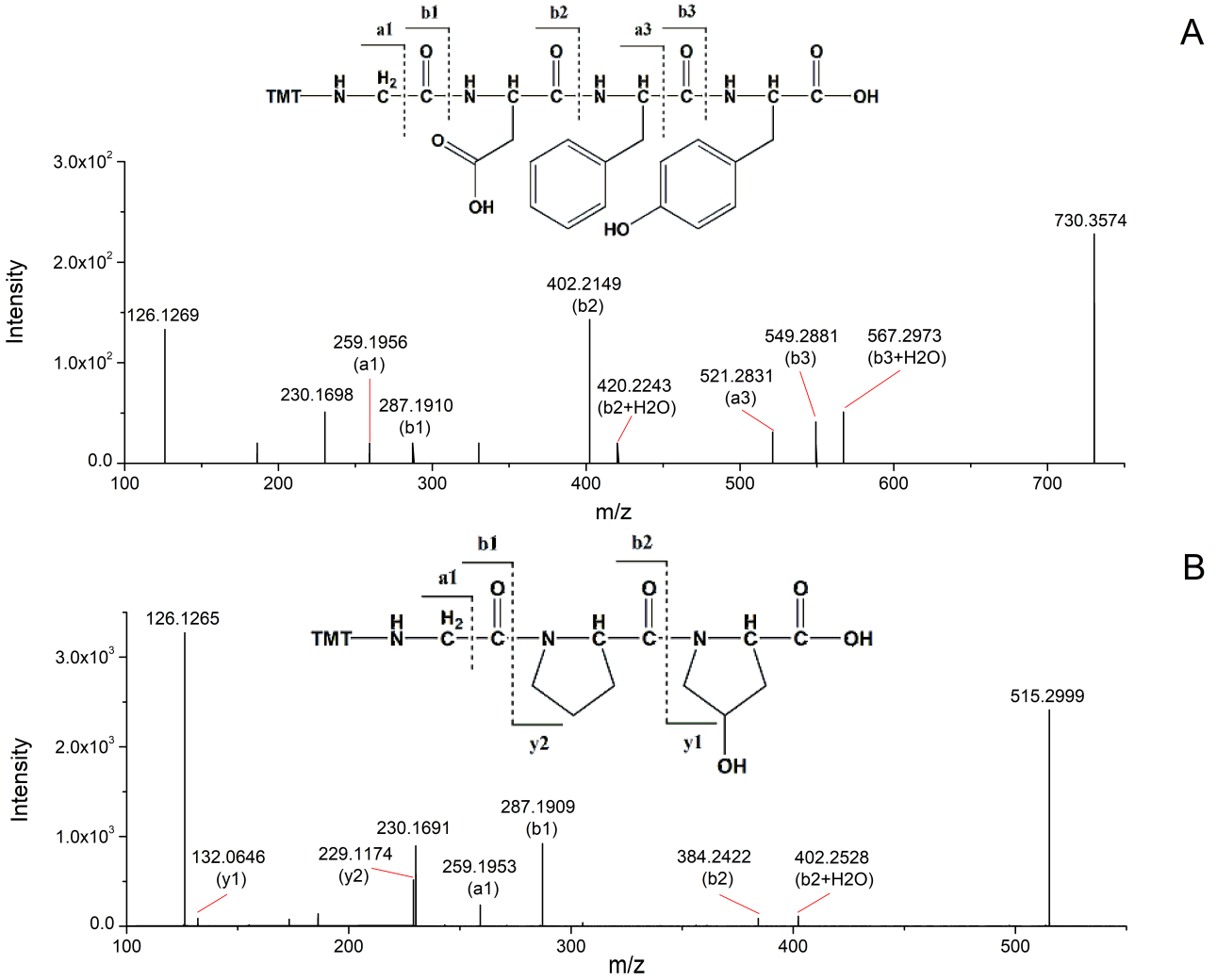


Figure 3. MS/MS spectra of TMT-labeled Gly-Asp-Phe-Tyr (**A**) and Gly-Pro-Hyp (**B**) oligopeptides.

Oligopeptides containing leucine or isoleucine were identified by comparison with standards. Specifically, as illustrated in Figure S3, the retention times of oligopeptides 18 and 21 matched those of the corresponding oligopeptide standards. Notably, oligopeptides containing multiple leucine or isoleucine residues were also identified via retention-time matching against authentic reference standards. The MS/MS spectra of all oligopeptides are shown in Figure S4.

4. Discussion

The oligopeptides screened and identified from pilose antler in this study were composed of two to five amino acid residues, with relative molecular masses predominantly distributed between 200 and 500 Da. This molecular weight distribution is highly consistent with the recognized characteristic range (200–600 Da) of natural pilose antler oligopeptides reported in previous pharmacological and compositional studies [16], confirming that the compounds identified in the present work are typical endogenous active oligopeptide

components of pilose antler and supporting the reliability of our sample pretreatment and identification system.

Jingfeng Li identified 18 oligopeptides and four amino acid constituents from the animal-derived Chinese medicine tortoise shell using label-free two-dimensional liquid chromatography mass spectrometry [17]. However, such label-free analytical methods have inherent technical drawbacks, including cumbersome separation steps, prolonged detection cycles, low detection sensitivity, and poor retention of highly polar small-molecule peptides on reversed-phase columns, which can easily lead to the omission of trace active oligopeptides and restrict the comprehensive exploration of active components in animal-derived medicinal materials. To address the above technical bottlenecks, this study established an efficient qualitative identification strategy integrating TMT labeling technology with UHPLC-Q-Orbitrap/MS. Compared with traditional label-free methods, this optimized analytical workflow exhibits prominent methodological advantages. On the one hand, TMT derivatization effectively reduces the polarity of native oligopeptides and amino acid molecules, significantly enhancing their retention behavior on reversed-phase chromatographic columns and improving chromatographic separation resolution. On the other hand, the combination of high-precision Orbitrap mass spectrometry and TMT labeling not only shortens the overall analytical cycle and improves experimental efficiency but also greatly enhances the detection coverage and sensitivity for highly polar, low-abundance oligopeptide and amino acid components. This technical improvement compensates for the loss of components associated with traditional detection methods, enables more comprehensive mining of low-molecular-weight active oligopeptides in pilose antler, and provides a reliable technical reference for the compositional analysis of other homologous animal-derived traditional Chinese medicines.

While direct experimental research on pilose antler oligopeptides remains limited, several oligopeptides identified in this study have been documented to exhibit distinct biological activities and pharmacological properties. The oligopeptide Gly-Pro-Hyp exerts chemotactic effects on fibroblasts and peripheral blood neutrophils [18], and has been validated as a high-efficiency collagen-derived oligopeptide with anti-photoaging activity [19]. This bioactivity suggests that Gly-Pro-Hyp may mediate skin tissue repair and protection against oxidative damage, which partially explains the traditional efficacy of pilose antler in nourishing and repairing tissues. In addition, the Ala-Tyr oligopeptide has shown good biosafety with no observable cytotoxicity within the concentration range of 100–800 μmol·L, and can effectively promote melanin synthesis at optimal concentrations [20], implying its potential application value in regulating melanocyte physiological function. Furthermore, Leu–Ile has been shown to upregulate the expression of brain-derived neurotrophic factor and glial cell line-derived neurotrophic factor in the retina via periocular delivery, thereby potentially improving the survival rate of retinal ganglion cells following optic nerve injury [21]. This neuroprotective effect reveals the potential of pilose antler oligopeptides in nervous system protection and nerve injury repair.

Collectively, the diverse biological activities of these identified oligopeptides preliminarily elucidate the material basis for the multiple pharmacological effects of pilose antler. More importantly, the optimized TMT-UHPLC-Q-Orbitrap/MS method established in this study provides an efficient and accurate technical platform for the in-depth exploration of active oligopeptides in pilose antler.

5. Conclusions

This study established an analytical method for oligopeptide identification using TMT labeling coupled with UHPLC-Q-Orbitrap/MS, which was successfully applied to analyze

oligopeptides derived from pilose antler. A total of 26 amino acids and 33 oligopeptides (comprising two to five amino acid residues) were identified.

Supplementary Materials: The following supporting information can be downloaded at: https://www.mdpi.com/article/10.3390/separations13100288/s1, Figure S1: The workflow of this study and the TMT labeling reaction process; Figure S2: Extracted ion chromatograms of TMT labled amino acid standards (A) and pilose antler extracts (B); Figure S3: Extracted ion chromatograms of TMT labled oligopeptide standards (A) and pilose antler extracts (B); Figure S4: Tandem mass spectra of Oligopeptide No.1-33; Table S1: Information of Pilose Antler Decoction Piece Samples.

Author Contributions: Conceptualization, S.G.; Methodology, S.G.; Software, M.D.; Validation, M.D.; Writing—review & editing, L.L.; Project administration, Data curation and Visualization, H.Z.; Supervision, L.L.; Funding acquisition, L.L. All authors have read and agreed to the published version of the manuscript.

Funding: This study was supported by grants from the Science and Technology Project of the Department of Science and Technology of Jilin Province (Grant No. YDZJ202201ZYTS268).

Data Availability Statement: The datasets supporting the findings of this study are available within the article and its Supplementary Materials.

Conflicts of Interest: The authors declare no conflict of interest.

References

1. Du, F.; Zhao, H.; Yao, M.; Yang, Y.; Jiao, J.; Li, C. Deer antler extracts reduce amyloid-beta toxicity in a Caenorhabditis elegans model of Alzheimer's disease. *J. Ethnopharmacol.* **2021**, *285*, 114850. [CrossRef] [PubMed]
2. Wang, F.; He, G.; Liu, M.; Sun, Y.; Ma, S.; Sun, Z.; Wang, Y. Pilose antler extracts promotes hair growth in androgenetic alopecia mice by activating hair follicle stem cells via the AKT and Wnt pathways. *Front. Pharmacol.* **2024**, *15*, 1410810. [CrossRef] [PubMed]
3. Wu, F.; Li, H.; Jin, L.; Li, X.; Ma, Y.; You, J.; Li, S.; Xu, Y. Deer antler base as a traditional Chinese medicine: A review of its traditional uses, chemistry and pharmacology. *J. Ethnopharmacol.* **2013**, *145*, 403–415. [CrossRef] [PubMed]
4. Wang, G.; Meng, Y.; Ouyang, W.; Zhao, C.; Zhao, W. Effect of pilose antler polypeptide on the mechanism of bone homeostasis in osteoporosis. *Front. Med.* **2023**, *10*, 1289843. [CrossRef] [PubMed]
5. Hu, Y.; Zhao, M.; Zhao, T.; Qi, M.; Yao, G.; Dong, Y. The Protective Effect of Pilose Antler Peptide on CUMS-Induced Depression Through AMPK/Sirt1/NF-κB/NLRP3-Mediated Pyroptosis. *Front. Pharmacol.* **2022**, *13*, 815413. [CrossRef] [PubMed]
6. Ni, Y.; Wang, Z.; Ma, L.; Yang, L.; Wu, T.; Fu, Z. Pilose antler polypeptides ameliorate inflammation and oxidative stress and improves gut microbiota in hypoxic-ischemic injured rats. *Nutr. Res.* **2019**, *64*, 93–108. [CrossRef] [PubMed]
7. Wang, X.; Chen, Y.; Cheng, Z.; Cao, Z.; Cheng, S.; Xin, C.; Zhang, J.; Zhang, F.; Chen, Y.; Wang, J.; et al. Pilose Antler Peptide Enhances Diabetic Fracture Healing by Modulating the CREB-Smad2/3-Runx2 Signaling Axis. *J. Ethnopharmacol.* **2025**, *354*, 120514. [CrossRef] [PubMed]
8. Zheng, K.; Li, Q.; Lin, D.; Zong, X.; Luo, X.; Yang, M.; Yue, X.; Ma, S. Peptidomic analysis of pilose antler and its inhibitory effect on triple-negative breast cancer at multiple sites. *Food Funct.* **2020**, *11*, 7481–7494. [CrossRef] [PubMed]
9. Bian, X.; Li, J.; Sun, J.; Zhang, H. 1HNMR metabolomics of MC3T3-E mouse osteoblast proliferation and alkaline phosphatase content by deer antler peptide amine. *Chin. J. Anal. Chem.* **2021**, *49*, 103–109. [CrossRef]
10. Zhang, H.; Wu, N.; Sun, J.; Liu, D.; Guo, X. Preparation and Application of Pilose Antler Oligopeptide Enteric-Coated Microcapsules. China Patent CN104027352B, 3 November 2017. [PubMed]
11. Khavinson, V.; Linkova, N.; Kozhevnikova, E.; Dyatlova, A.; Petukhov, M. Transport of biologically active ultrashort peptides using POT and LAT carriers. *Int. J. Mol. Sci.* **2022**, *23*, 7733. [CrossRef] [PubMed]
12. Liao, R.; You, P.; Weng, K.; Li, L.; Song, Y. TMT Labeling under Acidic pH Overcomes Detrimental Overlabeling and Improves Peptide Identification Rates. *Anal. Chem.* **2023**, *95*, 10595–10602. [CrossRef] [PubMed]
13. Ruwolt, M.; Schnirch, L.; Borges Lima, D.; Nadler-Holly, M.; Viner, R.; Liu, F. Optimized TMT-Based Quantitative Cross-Linking Mass Spectrometry Strategy for Large-Scale Interactomic Studies. *Anal. Chem.* **2022**, *94*, 5265–5272. [CrossRef] [PubMed]
14. Lu, Y.; Zhang, Y.; Xia, Y.; Huo, X.; Hua, M.; Sun, Y.-S. Quality assessment of different forms of Cervi Cornu Pantotrichum based on content of free amino acids. *China J. Chin. Mat. Med.* **2022**, *47*, 1587–1594. [CrossRef] [PubMed]
15. Ma, S.; Li, F.; Tian, Z.; Wu, J.; Wang, S.; Li, Q.; Wang, F. Analysis of Amino Acid Composition in New Zealand Velvet Antler Slices. *Chin. Arch. Tradit. Chin. Med.* **2020**, *38*, 69–73.

16. Wang, H.; Lin, Z.; Liu, Q.; Cai, M.; Xu, L.; Zhang, X. Preparation of Velvet Antlers Small Peptides and Stimulating Effects on Osteosarcoma Cell Proliferation. *Chem. J. Chin. Univ.* **2008**, *29*, 1791–1796.
17. Li, J. Peptide Composition of Tortoise Shell and Its Mechanism of Bone Strengthening. Ph.D. Thesis, Changchun University of Chinese Medicine, Changchun, China, 2020.
18. Won, J.; Kang, J.; Noh, K.; Chung, H.-C.; Kang, W. Pharmacokinetics of collagen dipeptides (Gly-Pro and Pro-Hyp) and tripeptides (Gly-Pro-Hyp) in rats. *J. Food Sci.* **2024**, *89*, 701–709. [CrossRef] [PubMed]
19. Yang, D.; Liu, Q.; Xu, Q.; Zheng, L.; Zhang, S.; Lu, S.; Xiao, G.; Zhao, M. Effects of collagen hydrolysates on UV-induced photoaging mice: Gly-Pro-Hyp as a potent anti-photoaging peptide. *Food Funct.* **2024**, *15*, 3008–3022. [CrossRef] [PubMed]
20. Fan, Y.; Wei, J.; Li, Z.; Yang, J.; Hu, X.; Zhang, H. Biosynthesis, Characterization, and Bioactivity of L-Alanyl-L-tyrosine in Promoting Melanin Synthesis. *Appl. Biochem. Biotechnol.* **2024**, *196*, 3693–3707. [CrossRef] [PubMed]
21. Nakatani, M.; Shinohara, Y.; Takii, M.; Mori, H.; Asai, N.; Nishimura, S.; Furukawa-Hibi, Y.; Miyamoto, Y.; Nitta, A. Periocular injection of in situ hydrogels containing Leu-Ile, an inducer for neurotrophic factors, promotes retinal ganglion cell survival after optic nerve injury. *Exp. Eye Res.* **2011**, *93*, 873–879. [CrossRef] [PubMed]

Disclaimer/Publisher's Note: The statements, opinions and data contained in all publications are solely those of the individual author(s) and contributor(s) and not of MDPI and/or the editor(s). MDPI and/or the editor(s) disclaim responsibility for any injury to people or property resulting from any ideas, methods, instructions or products referred to in the content.